ELSEVIER

Energy transfer to Ce^{3+} ions in $Tb_3Al_5O_{12}$: Ce single crystalline films

Y. Zorenko[a], T. Voznyak[a], V. Vistovsky[a], T. Zorenko[a], S. Nedilko[b], M. Batentschuk[c],
A. Osvet[c], A. Winnacker[c,*], G. Zimmerer[d], V. Kolobanov[e], D. Spassky[e]

[a]*Department of Electronic Ivan Franko National University of Lviv, 79017 Lviv, Ukraine*
[b]*Physical Faculty of Kyiv National Taras Shevchenko University, 03680 Kyiv, Ukraine*
[c]*Department of Materials Sciences 6, University of Erlangen-Nuernberg, D 91058 Erlangen, Germany*
[d]*II Institute of Experimental Physics, University of Hamburg, D 22761 Hamburg, Germany*
[e]*Physical Faculty of Moscow State University, 119992 Moscow, Russia*

Abstract

Existence of effective energy transfer from matrix (Tb^{3+} cations) to Ce^{3+} ions has been shown in TbAG:Ce single crystalline films (SCF) by means of investigation of the time-resolved emission and excitation spectra as well as luminescence decay under excitation by synchrotron radiation.
© 2007 Elsevier Ltd. All rights reserved.

Keywords: Garnets; Ce^{3+} dopant; Luminescence; Energy transfer

1. Introduction

$Tb_3Al_5O_{12}$ (TbAG) garnet is a suitable material for Faraday effect optical isolators (Chani et al., 2000) and for luminescent converters in light-emitting diodes (LED) (Kummer et al., 2001; Batentschuk et al., 2004). Compared with LuAG:Ce and YAG:Ce, the Ce^{3+} emission spectrum in TbAG:Ce is significantly shifted to the red side due to the reduced local symmetry of the Ce ions in the dodecahedral sites of the garnet lattice (Batentschuk et al., 2004). For this reason, growth of TbAG:Ce single-crystalline film (SCF) scintillators can be prospective for the development of screens for visualization of X-ray images (Koch et al., 1999; Globus et al., 2004; Zorenko et al., 2006). The advantage of these screens would be a good overlap of the emission spectrum of the SCF and the sensitivity range of CCD detectors (Zorenko et al., 2006).

In our previous paper (Zorenko et al., 1999, 2002; Koch et al., 1998) co-doping of $Y_3Al_5O_{12}$: Ce (YAG:Ce) and $Lu_3Al_5O_{12}$: Ce (LuAG:Ce) SCF by Tb^{3+} ions was used to increase the light yield (LY) of Ce^{3+} ions due to the possible energy transfer between Ce and Tb ions. We have shown (Zorenko et al., 2002; Koch et al., 1998) that the LY of LuAG:Ce,Tb SCF screens exceeds that of YAG:Ce and LuAG:Ce SCF by a factor of 1.5 and 1.35, respectively. The emission spectrum of LuAG:Ce,Tb SCF also matches better the spectral sensitivity region of CCDs (Zorenko et al., 2002; Koch et al., 1998). Another possible method of "engineering" of the luminescence spectra of Ce^{3+}-doped garnets is using the concentrated matrices based on rare earth (RE) elements where the efficient transfer of excitation energy can take place from the host cations to the activator ions. The TbAG is a well-known example of such concentrated matrices (Chani et al., 2000; Kummer et al., 2001; Batentschuk et al., 2004).

In TbAG:Ce garnet the presence of an effective energy transfer from the matrix (Tb^{3+} cations) to the Ce^{3+} activator has also been shown by Batentschuk et al. (2004). In this paper, we present the results of investigation of energy transfer from the host to the Ce^{3+} ions in TbAG:Ce SCF under excitation by synchrotron radiation (SR).

2. Experimental results and discussion

Growth of TbAG:Ce and undoped TbAG SCF was carried out by liquid phase epitaxy (LPE) on YAG substrate (details in
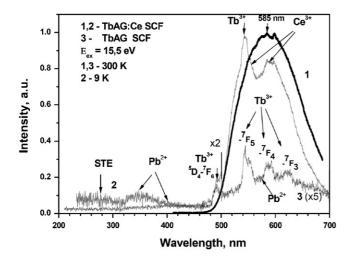
* Corresponding author.
  E-mail address: awinn@ww.uni-erlangen.de (A. Winnacker).

Fig. 1. The emission spectra of TbAG:Ce (1,2) and TbAG (3) SCF at 300 K (1,3) and 9 K (2) under excitation by SR with an energy of 15.5 eV.

Fig. 2. Excitation spectrum (1) of the Ce^{3+} ions emission at wavelength 590 nm in the TbAG:Ce SCF at 9 K. The reflection spectrum (2) of TbAG:Ce is shown for comparison.

Zorenko et al., 2006). Time-resolved emission and excitation spectra as well as kinetics of luminescence excited by SR in the UV–VUV region (3–25 eV) at 9 and 300 K were studied on Superlumi station in HASYLAB at DESY. The luminescence and excitation spectra were measured in the integral mode with repetition time of 200 ns. The fast component was detected in the time window of 5 ns with the 1.2 ns delay relative to the SR pulse with duration of 0.127 ns and repetition time of 200 ns. The slow component was detected in the 50 ns time window, delayed by 150 ns. The decay curves were measured in the time range of 0–200 ns at 9 and 300 K.

The luminescence spectra of TbAG:Ce and TbAG SCF at 300 and 9 K are shown on Fig. 1. Under SR excitation in the region of inter-band transitions ($E = 15.5$ eV, $\sim 2E_g$) the emission spectrum of TbAG:Ce SCF at 300 K (Fig. 1, curve 1) contains only the intense band of Ce^{3+} luminescence peaked at 585 nm. At low temperature the emission spectrum of TbAG:Ce SCF (Fig. 1, curve 2) presents two bands peaked at 545 and 595 nm which correspond to the radiative transition from the lowest energy doublet ($2t_g$) of $5d^1$ shell to the $^2F_{5/2,7/2}$ (4f) levels of the ground state of Ce^{3+} ions. It is worth noting that the emission spectrum of Ce^{3+} ions at 9 K, mainly the band at 545 nm, is modified by the TbAG host luminescence (Fig. 1, curve 3): the low-intensity sharp bands peaked at 490, 543 and 590 nm correspond to the $^5D_4 > {}^7F_j$ ($j = 6$–4) transitions of Tb^{3+} cations. The weak bands at 350 and 400 nm in the luminescence spectra of TbAG:Ce and TbAG SCF are caused by the X- and T-components of the short-wavelength emission band of Pb^{2+} ions as the main trace impurity in the LPE grown SCF (Zorenko et al., 2004a) whereas the long-wavelength emission bands of Pb^{2+} ions between 590 and 600 nm overlap with the emission of Ce ions (Fig. 1, curves 2 and 3). The very weak band in the UV (250–300 nm) range of TbAG:Ce SCF emission spectrum can be related to the luminescence of self-trapped excitons (STE) in the TbAG host. The STE emission is known to have similar position in YAG and LuAG SCF (Zorenko et al., 2004a, b, 2005a, b).
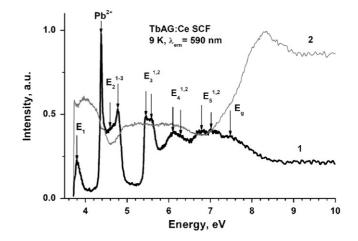
The excitation spectrum of the Ce^{3+} emission at 590 nm in the TbAG:Ce SCF at 9 K (curve 1) and reflection spectrum (curve 2) are shown in Fig. 2. The whole excitation spectrum of the Ce^{3+} luminescence in TbAG:Ce SCF with the exception of the sharp line peaked at 4.37 eV corresponds to the $4f^8 > 4f^7 5d^1$ transition of the Tb^{3+} ions. This confirms the existence of the efficient energy transfer between the TbAG host and the Ce^{3+} ions.

The $4f^8$ configuration of Tb^{3+} has the ^7F_j ground states, which split into seven levels due to the spin–orbit interaction. The 5d levels of Tb^{3+} ions at the dodecahedral sites of garnet lattice with D_2 symmetry are split into five $E(i=1$–5) levels due to the crystal field (Fig. 2). Each of these levels splits into $^9E(i)$ and $^7E(i)$ levels by the spin orbital coupling. Without overlap, we should observe 10 bands following alternately with spin degeneracy of 9 and 7 (Dorenbos, 2000). The transitions between the ^7F ground state of Tb^{3+} and 5d levels are alternately strong (^7E) and weak (^9E) due to the spin selection rule ($\Delta S = 0$). In the case of TbAG:Ce SCF, the excitation spectrum of Ce^{3+} ions consists of at least nine $E_{1–5}$ bands (Fig. 2) corresponding to the $^7F_j > {}^7E$ and $^7F_j > {}^9E$ transitions. The spectral position of these bands and indication of the above-mentioned transitions are shown in Table 1. The band E_g peaked at 7.47 eV is caused by the interband transition in the TbAG host. The sharp line at 4.37 eV (283 nm) probably corresponds to the $^1S_0–{}^3P_1$ transition of the Pb^{2+} trace impurity. The absorption band corresponding to this transition of Pb^{2+} ions is known to have a close position in YAG and LuAG SCF (Zorenko et al., 1999, 2002).

The decay kinetics of luminescence of TbAG:Ce SCF at 9 and 300 K is shown in Fig. 3a and b, respectively. The form of the decay curves depends on the energy of SR excitation. Under excitation by SR with energy of 5.63 eV in the E_3 band of Tb^{3+} ions (Fig. 2, curve 1) the luminescence decay of Ce^{3+} ions (Fig. 3a, curve 2) can be presented by a superposition of two components: the main fast component with a lifetime of 41.6 ns (33.4% of the initial amplitude) and slow component

Table 1
Positions of excitation bands of Ce^{3+} ions luminescence in TbAG:Ce SCF at 9 K and corresponding to them transitions

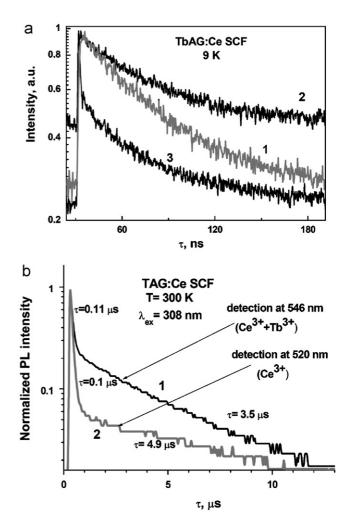| Indication of bands	Energy (eV)	Transition
E_1	3.79	$^7F_j \, (4f^8) > \, ^9E(4f^7d^1) \, (Tb^{3+})$
Pb^{2+}	4.37	$^1S_0 > \, ^3P_1 \, (Pb^{2+})$
E_2^1	4.60	$^7F_j \, (4f^8) > \, ^7E(4f^7d^1), \, ^9T_2(4f^7d^1) \, (Tb^{3+})$
E_2^2	4.775	$^7F_j \, (4f^8) > \, ^7T_2(4f^7d^1) \, (Tb^{3+})$
E_3^1	5.45	$^7F_j \, (4f^8) > \, ^7E(4f^7d^1) \, (Tb^{3+})$
E_3^2	5.58	$^7F_j \, (4f^8) > \, ^9E(4f^7d^1) \, (Tb^{3+})$
E_4^1	6.095	$^7F_j \, (4f^8) > \, ^7E(4f^7d^1) \, (Tb^{3+})$
E_4^2	6.26	$^7F_j \, (4f^8) > \, ^9E(4f^7d^1) \, (Tb^{3+})$
E_5^1	6.80	$^7F_j \, (4f^8) > \, ^7E(4f^7d^1) \, (Tb^{3+})$
E_5^2	7.01	$^7F_j \, (4f^8) > \, ^9E(4f^7d^1) \, (Tb^{3+})$
E_g	7.46	$Tb^{3+} > Tb^{4+} + e$

Fig. 3. Decay of TbAG:Ce SCF emission at wavelength of 560 nm under SR excitation with photon energy of 4.37 (1), 5.63 (2) and 15.5 eV (3) at 9 K; and (b) luminescence decay of TbAG:Ce SCF under excimer laser excitation with an energy of 4.02 eV (308 nm) at 300 K, detected at the Ce^{3+} (1) and Ce^{3+}–Tb^{3+} (2) emission bands.

(56.6%) with a lifetime of 600 ns. The first component of emission corresponds to the Ce^{3+} ions luminescence, the slow component is caused by the energy transfer between the Tb^{3+} cations and Ce^{3+} ions. The fraction of the slow component in the emission of TbAG:Ce SCF decreases up to 31.4% (Fig. 3a, curve 1) when the luminescence of Ce^{3+} ions is excited by SR with the energy of 4.37 eV which corresponds to the maximum of the Pb^{2+} ions excitation band (Fig. 2, curve 2; table). Such acceleration of the emission decay of Ce^{3+} ions under excitation in the 4.37 eV band probably is related to the existence of effective energy transfer from Pb^{2+} to Ce^{3+} ions at 9 K, which also has been found for LuAG:Ce SCF (Babin et al., 2007).

Under excitation by SR in the region of band-to-band transition the decay curves of Ce^{3+} emission in TbAG:Ce SCF (Fig. 3a, curve 3) can be fitted by superposition of the three components: $I(t) = 0.045 + 0.34 \exp(-t/0.8 \, \text{ns}) + 0.26 \exp(-t/47.5 \, \text{ns}) + 0.25 \exp(-t/560 \, \text{ns})$. It should be noted that the ultra-fast component with $\tau_1 = 0.8$ ns in the Ce^{3+} ions luminescence is comparable with the duration of SR pulse, therefore we do not draw any conclusion in this work regarding the presence and magnitudes of this component. The components with a lifetimes $\tau_1 = 47.5$ and 558 ns correspond to the 'intrinsic' Ce^{3+} ions emission and process of $Tb^{3+} \rightarrow Ce^{3+}$ energy transfer in TbAG host, respectively.

Due to the short (200 ns) detection range of the decay under excitation by SR we also studied the emission of the TbAG:Ce SCF at 300 K under the excitation of an excimer laser with an energy of 4.02 eV (308 nm; pulse duration 25 ns). The emission of Ce^{3+} was detected at the wavelength of 520 nm and the combined emission of Ce^{3+} and Tb^{3+} ions at a wavelength of 546 nm (Fig. 3b, see also Fig. 1).

The luminescence decay of Ce^{3+} at 520 nm can be presented by a sum of two components: fast one with a decay time of 0.1 μs (87% of initial amplitude) and slow one with a decay time of 4.9 μs (13%). The order of magnitude of the lifetime of fast components in curves excited by excimer laser is the same as in the curves measured under SR excitation at 9 K (Fig. 3a, curves 1–3).

The slow component is longer under the excitation by excimer laser. The relative intensity of the slow component is significantly higher when the detection wavelength is tuned from 520 to 546 nm. At this wavelength the emission of Ce^{3+} ions is detected simultaneously with the $^5D_4$–$^7F_5$ emission Tb^{3+} ions (Fig. 3b, curve 2). We interpret the fast component as the emission of Ce^{3+} ions excited directly, and the slow component as the lifetime of the Tb^{3+} subsystem, which reveals itself in the Ce^{3+} emission as a result of energy transfer. The 546 nm decay curve can be fitted by the superposition of two components with a lifetime of 0.11 μs (65%) and 3.5 μs (35%). Due to the close values of the fast and slow components of emission related to Ce^{3+} and both Ce^{3+} and Tb^{3+} ions (Fig. 3b, curves 1 and 2, respectively), we conclude that the luminescence of Ce^{3+} ions in the TbAG host is largely determined by the nonradiative energy transfer from the Tb^{3+} cations.

Since the energy transfer from TbAG host to Ce^{3+} ions is characterized by the existence of two slow components, we conclude that the transfer to Ce^{3+} ions happens at different

excited levels of Tb^{3+} ions, depending on the excitation mechanism. Considering the energy levels of Ce^{3+} ions in TbAG host (Turos-Matysjak et al., 2007), we assume that after spin-allowed and spin-forbidden excitation of the $5d^1 4f^7$ states of Tb^{3+} ions and after relaxation to the $^5D_0$ and $^5D_3$ states of Tb^{3+}, the energy is transferred to the 5d excited levels of Ce^{3+}. Thus, two-component emission decay of Ce^{3+} in TbAG host with the lifetimes $\tau_1 = 0.56$–$0.6\,\mu s$ and $\tau_2 = 3.5$–$4.9\,\mu s$ can correspond to the non-radiative transitions from $^5D_3$ and $^5D_0$ states of Tb^{3+} ions to ^2E and $^2T_2$ levels of $5d^1$ configuration of Ce^{3+} ions. It is also noteworthy that the energy corresponding to the $^7F_j \rightarrow {}^5D_3$ and $^7F_j \rightarrow {}^5D_0$ transitions (3.29–3.35 and 3.99 eV, respectively) well overlaps with the energies of the 4f $(^2F_{5/2,7/2}) \rightarrow 5d^1$ (^2E and $^2T_2$) transitions (2.67 and 3.77 eV, respectively) (Zorenko et al., 2006).

3. Conclusion

The presence of the characteristic 4f–5d4f bands of Tb^{3+} ions corresponding to the $^7F_j \rightarrow {}^7E$ and $^7F_j \rightarrow {}^9E$ transitions in the excitation spectrum of Ce^{3+} and the presence of components with the lifetimes $\tau_1 = 0.56$–$0.6\,\mu s$ and $\tau_2 = 3.5$–$4.9\,\mu s$ in the Ce^{3+} luminescence decay indicate an existence of efficient energy transfer from the host (Tb^{3+} cations) to the Ce^{3+} ions in the TbAG:Ce SCF. Different excited levels of the ions, probably, the 4f $(^5D_0, {}^5D_3)$ states of Tb^{3+} ions and the $5d^1(^2E, {}^2T_2)$ states of Ce^{3+} ions are involved in the transfer. In addition to scintillators and screens for visualization of X-ray images (Zorenko et al., 2006), TbAG:Ce SCF can also be used as an effective thin-film luminescence converter of LED radiation in LUCOLED light devices. This conclusion is supported by the existence of the strong host excitation bands of Ce^{3+} luminescence in the 325–375 nm range corresponding to the E_1 and $^7F_6$–$^5D_3$ transitions of Tb^{3+} cations (Zorenko et al., 2006) in the region of radiation of typical UV LEDs.

Acknowledgments

References

Babin, V., Gorbenko, V., Makhov, A., Nikl, M., Zazubovich, S., Zorenko, Y., 2007. The role of Pb^{2+} ions in the luminescence of LuAG:Ce single crystalline films. Radiat. Meas., in press.

Batentschuk, M., Osvet, A., Schierning, G., Klier, A., Schneider, J., Winnacker, A., 2004. Simultaneous excitation of Ce^{3+} and Eu^{3+} ions in $Tb_3Al_5O_{12}$. Radiat. Meas. 38, 539–543.

Chani, V.I., Yoshikawa, A., Machida, H., Fukuda, T., 2000. (Tb, Yb)$_3$Al$_5$O$_{12}$ garnet: crystal-chemistry and fiber growth by micro-pulling-down technique. Mater. Sci. and Engineer. B 75, 53–60.

Dorenbos, P., 2000. The $4f^n \leftrightarrow 4f^{n-1}5d$ transitions of the trivalent lanthanides in halogenides and chalcogenides. Journal of Luminescence 91, 91–106.

Globus, M., Grinyov, B., Ratner, M., Tarasov, V., Lyubinskiy, V., Vydai, Yu., Ananenko, A., Zorenko, Yu., Gorbenko, V., Konstankevych, I., 2004. New type of scintillation detectors for biological, medical, and radiation monitoring applications. IEEE Trans. Nucl. Sci. 51, 1297–1303.

Koch, A., Raven, C., Spanne, P., Snigirev, A., 1998. X-ray imaging with submicrometer resolution employing transparent luminescent screens. J. Opt. Soc. Am. A 15 (N7), 1940–1951.

Koch, A., Peyrin, F., Heurtier, P., Chambaz, B., Ferrand, B., Ludwig, W., Couchaud, M., 1999. An X-ray camera for computed microtomography of biological samples with micrometer resolution using $Lu_3Al_5O_{12}$ and $Y_3Al_5O_{12}$ scintillators. Proc. SPIE 3659, 170–179.

Kummer, F., Zwaschka, F., Ellens, A., Debray, A., Waitl, G., 2001. Luminous substance for a light source and light source associated therewith. Intern. Patent Appl. No: WO 01/08452.

Turos-Matysjak, R., Gryk, W., Grinberg, M., Lin, Y.S., Liu, R.S., 2007. $Tb^{3+} \rightarrow Ce^{3+}$ energy transfer in $Y_{3-x-y}Tb_yGd_xAl_5O_{12}$ ($x = 0.65$, $y = 0.575$) doped Ce^{3+}, Radiat. Meas., in this volume, doi: 10.1016/j.radmeas.2007.02.003.

Zorenko, Yu., Batenshchuk, M., Gorbenko, V., Pashkovsky, M., Konstankevych, I., 1999. The factors determining the light yield of luminophors based on single crystalline films of Al_2O_3–Y_2O_3–R_2O_3 oxide compounds. Journal of Appl. Spectr. 66, 819–824.

Zorenko, Yu., Gorbenko, V., Konstankevych, I., Grinev, B., Globus, M., 2002. Scintillation properties of $Lu_3Al_5O_{12}$:Ce single crystalline films. NIM A486, 309–314.

Zorenko, Y.V., Konstankevych, I.V., Mikhailin, V.V., Kolobanov, V.N., Spasskii, D.A., 2004a. Luminescence of excitons in single-crystal garnets. Optics and Spectroscopy 96, 390–397.

Zorenko, Y., Voloshinovskii, A., Konstankevych, I., Kolobanov, V., Mikhailin, V., Spassky, D., 2004b. Luminescence of excitons and antisite defects in the phosphors based on garnet compounds. Radiat. Meas. 38, 677–680.

Zorenko, Y., Gorbenko, V., Konstankevych, I., Voloshinovskii, A., Stryganyuk, G., Mikhailin, V., Kolobanov, V., Spassky, D., 2005a. Single-crystalline films of Ce-doped YAG and LuAG phosphors: advantages over bulk crystals analogues. Journal of Luminescence 114 (N4), 85–94.

Zorenko, Yu., Gorbenko, V., Voloshinovskii, A., Stryganyuk, G., Mikhailin, V., Kolobanov, V., Spassky, D., Nikl, M., Blazek, K., 2005b. Exciton-related luminescence in LuAG:Ce single crystals and single crystalline films. Phys. Stat. Sol. (a) 202, 1113–1118.

Zorenko, Yu., Gorbenko, V., Konstankevych, I., Savchyn, V., Zorenko, T., Nedilko, S., Batenchuk, M., Osvet, A., Winnacker, A., Zimmerer, G., 2006. Growth and scintillation properties of single crystalline films of $Tb_3Al_5O_{12}$:Ce garnet. In: Proceedings of the SCINT 2005. Kharkiv, pp. 219–222.